Sensitivity of nuclear matrix elements of $0\nu\beta\beta$ of ^{48}Ca to different components of the two-nucleon interaction

Shahariar Sarkar,* Pawan Kumar, Kanhaiya Jha, and P. K. Raina
Indian Institute of Technology Ropar, Rupnagar, Punjab-140001, India

(Received 22 August 2019; revised manuscript received 12 November 2019; published 9 January 2020)

In the present work, we examine the sensitivity of nuclear matrix elements (NMEs) for light neutrino-exchange mechanism of neutrinoless double beta decay ($0\nu\beta\beta$) of ^{48}Ca to the central, spin-orbit, and tensor components of two-nucleon interaction. The NMEs are calculated in the nuclear shell-model framework in fp-model space using frequently used GXPF1A interaction and a new effective interaction named GX1R of pf shell. The decomposition of the shell-model two-nucleon interactions into their individual components is performed using spin-tensor decomposition. The NMEs are calculated in closure approximation by using optimal value of the closure energy. The results shows that the total NMEs calculated with the central component of the interactions are of positive sign. By adding spin-orbit part to central part of the interactions, sign of the total NMEs gets change, and in absolute value, NMEs decreases by about 15–18%. Sign change in total NMEs are again seen by adding tensor part to the central+spin−orbit part of the interactions. Similar trends of sign change are also observed for Fermi, Gamow-Teller, and tensor matrix elements. Thus we infer that SO and T part mostly cancel the effects of each other in NMEs calculations. For both the interactions, the total NMEs calculated with the C part is found to be 20% enhanced as compared to the NMEs calculated with the total interactions. With new GX1R interaction, there is about 1–3% increments in the total NMEs as compared to NMEs with GXPF1A interaction. This increments comes from the modifications of isospin $T = 1$ tensor force two-nucleon matrix elements to bring the characteristic properties of tensor force into the GX1R interaction.

DOI: 10.1103/PhysRevC.101.014307

I. INTRODUCTION

A long-standing fundamental problem of the particle physics is to determine whether neutrinos are Majorana fermion or Dirac fermion. The neutrinoless double beta decay ($0\nu\beta\beta$) process is of a particular importance in this respect. If this process is observed, then one can conclude that neutrinos are Majorana fermions [1]. This process also puts some light on the absolute mass of neutrino and neutrino mass hierarchy [2,3], which has huge implications in the physics beyond the standard model [1,4,5]. Various decay mechanisms such as light neutrino-exchange mechanism [6,7], heavy neutrino-exchange mechanism [8], left-right symmetric mechanism [9,10], and supersymmetric particles exchange mechanism [11,12] have been proposed for $0\nu\beta\beta$. In general, the decay rate in each mechanism is related to the nuclear matrix elements (NMEs) and absolute neutrino mass. These NMEs are calculated using theoretical nuclear many-body models [13]. In literature, the nuclear models such as the quasiparticle random phase approximation [8], the interacting shell model [14–18], the interacting boson model [19,20], the generator coordinate method [21], the energy density-functional theory [21,22] and the projected Hartree-Fock Bogolibov model [23], etc., have been used to calculate NMEs.

In the present work, NMEs for ^{48}Ca are calculated for light neutrino-exchange mechanism of $0\nu\beta\beta$. The $0\nu\beta\beta$ process for ^{48}Ca is written as

$$^{48}\mathrm{Ca} \rightarrow {}^{48}\mathrm{Ti} + e^- + e^-. \tag{1}$$

In Refs. [15–18], NMEs for the light neutrino-exchange mechanism of ^{48}Ca are calculated in the nuclear shell-model framework. However, NMEs in those studies are calculated using the total two-nucleon interaction. In recent years, the contribution of individual components, i.e., central (C), spin-orbit (SO), and tensor force (T), of shell-model two-nucleon interaction in the single-particle energy gaps have been explored to understand the cause of shell evolution in neutron-rich nuclei [24–28]. These studies, thus, motivate us to investigate the effects of individual components of two-nucleon interaction on the NMEs of $0\nu\beta\beta$.

The decomposition of effective shell-model interaction into its C, SO, and T force components are performed using spin-tensor decomposition (STD) [28–37]. The STD can be applied only when the spin-orbital partners, $j_>(= l + 1/2)$ and $j_<(= l - 1/2)$, associated with the same orbital quantum number l is present in the model space. Except ^{48}Ca, which belongs to pf shell, most of the other candidates of $0\nu\beta\beta$ belong to the higher-mass region, and the chosen model space for them do not have spin-orbital partners. Therefore, the present study for ^{48}Ca is of great interest.

*shahariar.sarkar@iitrpr.ac.in

In the present work, we examine the sensitivity of NMEs of ^{48}Ca to C, SO, and T components of GXPF1A interaction [38,39] and a new interaction GX1R [40] of pf shell. NMEs are calculated in the closure approximation by using the optimal value of closure energies ($\langle E\rangle$) in the denominator of neutrino potential, which takes care of the effects of excitation energy of a large number of states of the virtual intermediate nucleus (^{48}Sc in our case).

This paper is organized as follows. In Sec. II, the theoretical formalism to calculate NMEs for the light neutrino-exchange mechanism of $0\nu\beta\beta$ is presented. The details of the employed effective shell-model interactions and the spin tensor-decomposition are given in Sec. III. The results and discussion are presented in Sec. IV. The summary of this work is given in Sec. V. The expression for the two-body matrix elements and the form factors used in the calculations are given in the Appendices.

II. NUCLEAR MATRIX ELEMENTS OF $0\nu\beta\beta$

The decay rate for light neutrino-exchange mechanism of $0\nu\beta\beta$ can be written as [3,8]

$$\left[T_{\frac{1}{2}}^{0\nu}\right]^{-1} = G^{0\nu}|M^{0\nu}|^2\left(\frac{m_{\beta\beta}}{m_e}\right)^2, \tag{2}$$

where $G^{0\nu}$ is a well-known phase-space factor [41], $M^{0\nu}$ is the nuclear matrix element, and $m_{\beta\beta}$ is the effective Majorna neutrino mass defined by the neutrino mass eigenvalues m_k and the neutrino mixing matrix elements U_{ek}:

$$\langle m_{\beta\beta}\rangle = \left|\sum_k m_k U_{ek}^2\right|. \tag{3}$$

The nuclear matrix element $M^{0\nu}$ can be expressed as the sum of Gamow-Teller ($M^{0\nu}_{\rm GT}$), Fermi ($M^{0\nu}_F$), and tensor ($M^{0\nu}_T$) matrix elements as [3]

$$M^{0\nu} = M^{0\nu}_{\rm GT} - \left(\frac{g_V}{g_A}\right)^2 M^{0\nu}_F + M^{0\nu}_T, \tag{4}$$

where g_V and g_A are the vector and axial-vector constant, respectively. $M^{0\nu}_{\rm GT}$, $M^{0\nu}_F$, and $M^{0\nu}_T$ matrix elements of the scalar two-body transition operator O^{α}_{12} of $0\nu\beta\beta$ can be expressed as the sum over the product of the two-body transition density (TBTD) and antisymmetric two-body matrix elements ($\langle k_1', k_2', JT|\tau_{-1}\tau_{-2}O^{\alpha}_{12}|k_1, k_2, JT\rangle_A$) [17]:

$$\begin{aligned} M^{0\nu}_{\alpha} = \langle f|\tau_{-1}\tau_{-2}O^{\alpha}_{12}|i\rangle = &\sum_{J,k_1'\leqslant k_2',k_1\leqslant k_2} \mathrm{TBTD}(f,i,J) \\ &\times\langle k_1', k_2', JT|\tau_{-1}\tau_{-2}O^{\alpha}_{12}|k_1, k_2, JT\rangle_A, \end{aligned} \tag{5}$$

where $\alpha = (F, GT, T)$, J is the coupled spin of two decaying neutrons or two final created protons, τ_- is the isospin annihilation operator, A denotes that the two-body matrix elements are obtained using antisymmetric two-nucleon wave functions, and k stands for the set of spherical quantum numbers $(n; l; j)$. In our case, $|i\rangle$ is 0^+ ground state (g.s.) of the parent nucleus ^{48}Ca, $|f\rangle$ is the 0^+ g.s. of the granddaughter nucleus ^{48}Ti, and k has the spherical quantum numbers for $0f_{7/2}$, $0f_{5/2}$, $1p_{3/2}$, and $1p_{1/2}$ orbitals.

The TBTD can be expressed as [17]

$$\mathrm{TBTD}(f,i,J) = \langle f||[A^+(k_1',k_2',J)\otimes\tilde{A}(k_1,k_2,J)]^{(0)}||i\rangle, \tag{6}$$

where

$$A^+(k_1',k_2',J) = \frac{[a^+(k_1')\otimes a^+(k_2')]^J_M}{\sqrt{1+\delta_{k_1'k_2'}}} \tag{7}$$

and

$$\tilde{A}(k_1,k_2,J) = (-1)^{J-M}A^+(k_1,k_2,J,-M) \tag{8}$$

are the two-particle creation and annihilation operators of rank J, respectively.

To evaluate TBTD, one needs a large number of two nucleon transfer amplitudes (TNA). TNA are calculated with large set of intermediate states $|m\rangle$ of the $(n-2)$ nucleons system (^{46}Ca in the present study), where n is number of nucleons for the parent nucleus. TBTD in terms of TNA is expressed as [17]

$$\begin{aligned} \mathrm{TBTD}(f,i,J) = &\sum_m \mathrm{TNA}(f,m,k_1',k_2',J_m) \\ &\times\mathrm{TNA}(i,m,k_1,k_2,J_m), \end{aligned} \tag{9}$$

where TNA are given by

$$\mathrm{TNA}(f,m,k_1',k_2',J_m) = \frac{\langle f||A^+(k_1',k_2',J)||m\rangle}{\sqrt{2J_0+1}}. \tag{10}$$

Here J_m is the spin of the allowed states of ^{46}Ca. J_0 is spin of $|i\rangle$ and $|f\rangle$. $J_m = J$ when $J_0 = 0$ [17].

The two-body matrix elements (TBMEs) are calculated with the following scalar two-particle transition operators of $0\nu\beta\beta$ containing spin and radial neutrino potential operators [16]:

$$\begin{aligned} O^{\rm GT}_{12} &= \tau_{1-}\tau_{2-}(\boldsymbol{\sigma_1}.\boldsymbol{\sigma_2})H_{\rm GT}(r), \\ O^F_{12} &= \tau_{1-}\tau_{2-}H_F(r), \\ O^T_{12} &= \tau_{1-}\tau_{2-}S_{12}H_T(r), \end{aligned} \tag{11}$$

where $S_{12} = 3(\boldsymbol{\sigma_1}.\hat{\mathbf{r}})(\boldsymbol{\sigma_2}.\hat{\mathbf{r}}) - (\boldsymbol{\sigma_1}.\boldsymbol{\sigma_2})$, $\mathbf{r} = \mathbf{r_1} - \mathbf{r_2}$, and $r = |\mathbf{r}|$ is the internucleon distance of the decaying nucleons. To calculate the TBMEs one needs the neutrino potential that enters into the radial matrix $\langle n', l'|H_\alpha(r)|n, l\rangle$. The neutrino potential for light-neutrino exchange mechanism of $0\nu\beta\beta$ considering the closure approximation is given by [16]

$$H_\alpha(r) = \frac{2R}{\pi}\int_0^\infty \frac{j_p(qr)h_\alpha(q^2)q\,dq}{q+\langle E\rangle}, \tag{12}$$

where $j_p(qr)$ is spherical Bessel function, $p = 0$ for $M^{0\nu}_{\rm GT}$ and $M^{0\nu}_F$, and $p = 2$ for $M^{0\nu}_T$, q is the neutrino momentum of Majorana neutrino, R is the radius of the parent nucleus, $\langle E\rangle$ is the closure energy, and $h_\alpha(q^2)$ is the form factors that incorporates the effects of higher-order currents (HOC) and finite nucleon size (FNS) [7]. Detailed expression for the TBME is given in the Appendix A. Form factors used in the calculation are given in the Appendix B.

The short-range nature of the two-nucleon interaction is taken care by multiplying relative harmonic oscillator wave function ψ_{nl} with a correlation function $f(r)$ [15]:

$$\psi_{nl}(r) \longrightarrow [1+f(r)]\psi_{nl}(r), \tag{13}$$

TABLE I. Parameters for the SRC parametrization of Eq. (14).

SRC type	a	b	c
Miller-Spencer	1.10	0.68	1.00
CD-Bonn	1.52	1.88	0.46
AV18	1.59	1.45	0.92

where $f(r)$ can be parametrized as [42]

$$f(r) = -ce^{ar^2}(1 - br^2). \tag{14}$$

The parameters a, b, and c for Miller-Spencer, Charge-Dependent Bonn (CD-Bonn), and Argonne V18 (AV18) type short-range correlation (SRC) parametrization are given in Table I [15].

After including SRC correlations, the radial matrix element of $H_\alpha(r)$ is written as [15]

$$\int_0^\infty \psi_{n'l'}(r)H_\alpha(r)\psi_{nl}(r)[1 + f(r)]^2 r^2 dr. \tag{15}$$

III. EFFECTIVE INTERACTION AND SPIN-TENSOR DECOMPOSITION

In the present work, we have considered two effective shell-model interactions of pf shell, namely GXPF1A and GX1R, for calculating NMEs. The GXPF1A has been widely used to study the spectroscopic properties of $20 \leqslant Z \leqslant 28$ nuclei. In the literature, this interaction has also been used to calculate NMEs for $0\nu\beta\beta$ of ^{48}Ca [15–17].

The GX1R is the newest interaction of the GX family and has been recently derived by K. Jha *et al.* [40]. In the derivation of GX1R interaction, all isospin $T = 1$ tensor force two-nucleon matrix elements and the single-particle energy of $p_{3/2}$ orbital are modified. The modification in $T = 1$ two-nucleon matrix elements is done in order to bring the systematic properties of the total angular momentum (J) averaged tensor force matrix elements

$$\bar{V}^T_{jj'}(\mathcal{T}) = \frac{\sum_J (2J+1) < jj'|V(\mathcal{T})|jj' >_{JT}}{\sum_J (2J+1)}, \tag{16}$$

into the GX1R interaction. The properties of $\bar{V}^T_{jj'}(\mathcal{T})$ matrix elements are as follows: $\bar{V}^T_{jj'}(\mathcal{T})$ is attractive for $j_<j'_>$ and $j_>j'_<$ configurations,[1] whereas it is repulsive for $j_>j'_>$ and $j_<j'_<$ configurations [44–46].

In GXPF1A and its other modified versions, for example, GXPF1B [47] and GX1B1 [40], the properties of $\bar{V}^T_{jj'}(\mathcal{T})$ are missing for 7 of 10 [40,44–46]. This particular problem has been ameliorated in the GX1R interaction using the spin-tensor decomposition.

The GX1R has been tested for the level structure of $^{47-54}$Ca isotopes; the evolution of $E(2_1^+)$ in Ca, Ti, Cr, Fe, and Ni isotopes; and the effect of softness of ^{56}Ni core in the level structure of ^{55}Co, ^{56}Ni, and ^{57}Ni. The overall description of GX1R is reasonable for the above-mentioned nuclei.

[1]Here $j_>(= l + 1/2)$ and $j_<(= l - 1/2)$.

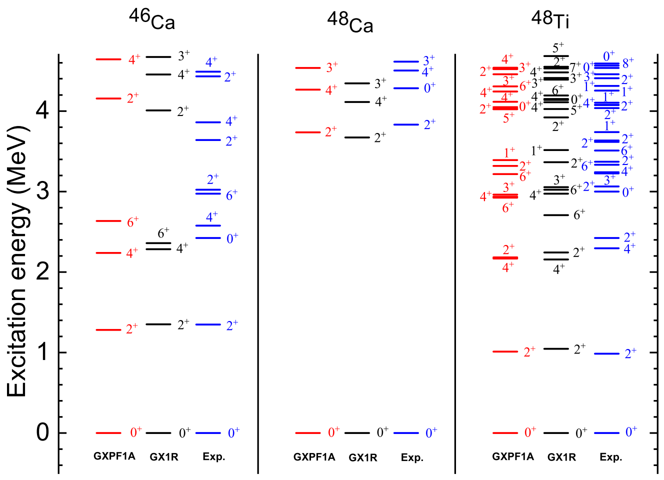

FIG. 1. Low-lying states of ^{46}Ca, ^{48}Ca, ^{48}Ti. Theoretical calculations are performed with GXPF1A and GX1R interactions. Experimental data are taken from Ref. [43].

The purpose of considering GX1R along with the GXPF1A for the present work is to test the validity of the GX1R interaction for calculating NMEs of $0\nu\beta\beta$ and to determine how much change will come in NMEs when the tensor force component of the two-nucleon interaction has its characteristic properties.

In Fig. 1, the calculated and the experimental low-lying energy levels of ^{46}Ca, ^{48}Ca, and ^{48}Ti are shown. The calculated energy levels are obtained with both GXPF1A and GX1R interactions. The results of both the interactions are found to be nearly the same, although the group of levels in ^{46}Ca and ^{48}Ca from 4 to 4.7 MeV predicted by GX1R are slightly shifted toward lower energy. With respect to experimental data, prediction of GX1R is also found to be satisfactory.

In the present study, we have employed spin-tensor decomposition [28–37] to decompose GXPF1A and GX1R interactions into their central (C), spin-orbit (SO), and tensor (T) force components. In spin-tensor decomposition, the interaction between two-nucleon is defined as the linear sum of the scalar product of configuration space operator Q and spin space operator S of rank k [30]:

$$V = \sum_{k=0}^{2} V(k) = \sum_{k=0}^{2} Q^k \cdot S^k, \tag{17}$$

where rank $k = 0$, 1, and 2 represent central, spin-orbit, and tensor force, respectively. Using the LS-coupled two-nucleon wave functions, the matrix element for each $V(k)$ can be calculated from the matrix element of V [29]:

$$\begin{aligned}\langle (ab), LS; J|V(k)|(cd), L'S'; J\rangle &= (2k+1)(-1)^J \\ &\times \begin{Bmatrix} L & S & J \\ S' & L' & k \end{Bmatrix} \sum_{J'} (-1)^{J'}(2J'+1) \begin{Bmatrix} L & S & J' \\ S' & L' & k \end{Bmatrix} \\ &\times \langle (ab), LS; J'|V|(cd), L'S'; J'\rangle,\end{aligned} \tag{18}$$

where a refers to the set of quantum numbers (n_a, l_a).

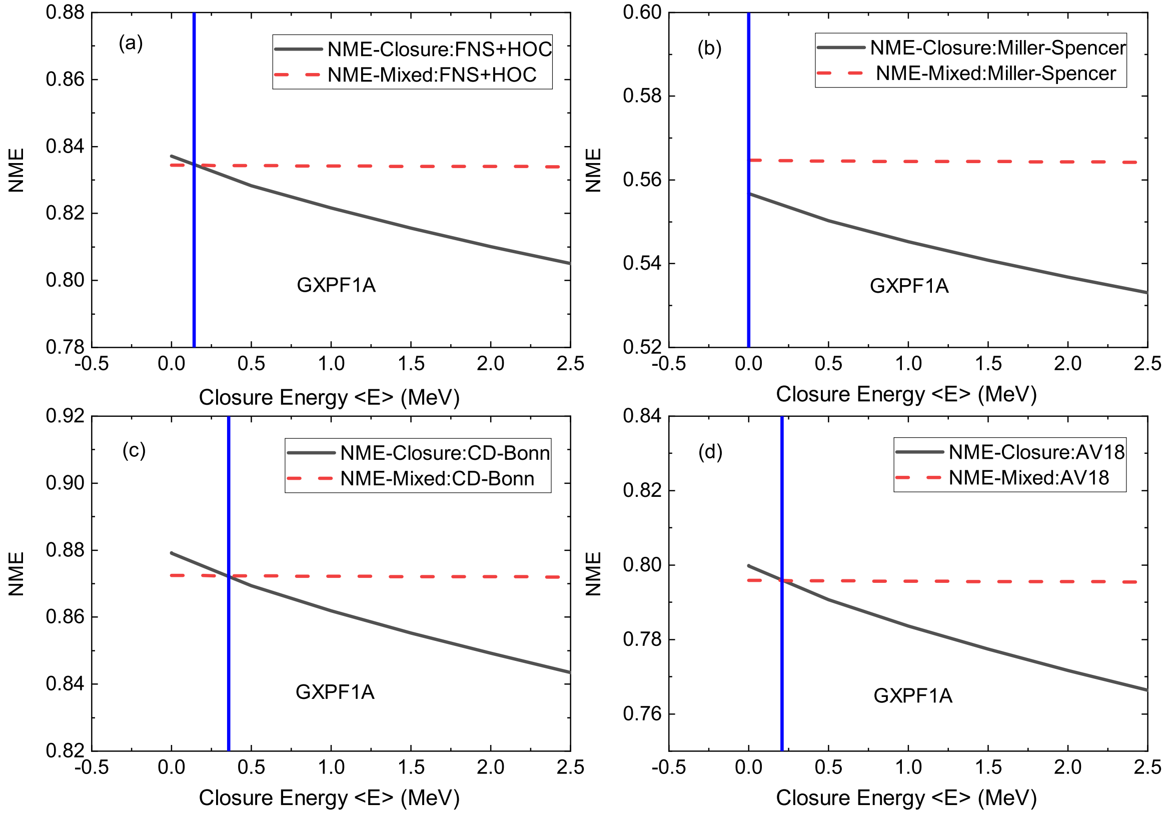

FIG. 2. Dependence of total closure and mixed NME for $0\nu\beta\beta$ (light neutrino-exchange mechanism) of ^{48}Ca on average closure energy $\langle E\rangle$, calculated with GXPF1A interaction for different SRC parametrization.

IV. RESULTS AND DISCUSSION

We have calculated the TBTD in terms of TNA using shell-model code NushellX@MSU [48]. The calculation of the required TBMEs has been done using the program written by us. We have considered the first 100 states of ^{46}Ca for each allowed spin-parity (J^{π}) to calculate TBTD. It is expected that the first 100 states may give TBTD with good accuracy and NMEs with almost constant value. A detailed description of the variation of NMEs with the number of states of ^{46}Ca is given latter in this section.

For the closure approximation, we have used the optimal value of the closure energy ($\langle E\rangle$). At the optimal $\langle E\rangle$, the NMEs calculated with the closure method and with the mixed method, described in Refs. [16,49–51], have the same value. The mixed method has fast NMEs convergence property, and it is the combination of three different methods, namely running nonclosure, running closure, and closure method.

In Ref. [16], the approximate value of the optimal $\langle E\rangle$ for the light neutrino-exchange mechanism of $0\nu\beta\beta$ was reported about 0.5 MeV for ^{48}Ca. However, the exact value is given in Fig. 3 of Ref. [49] where it is around 0.2 MeV. Value of the optimal $\langle E\rangle$ given in Refs. [16,49] was for GXPF1A interaction with CD-Bonn and AV18 SRC parametrizations.

For our calculations, we have extracted the optimal value of $\langle E\rangle$ for both GXPF1A and GX1R interactions with different SRC parametrizations by examining the dependence of closure and mixed NMEs of ^{48}Ca with $\langle E\rangle$. The running nonclosure and running closure part of the mixed method were performed using the formalism outlined in Ref. [16]. In these methods, the first 150 states of the intermediate nucleus (^{48}Sc) for each allowed spin-parity were considered to calculate the one body transition densities. The vector constant $g_V = 1$ and the axial-vector constant $g_A = 1.27$ were used. The closure method part of the mixed method was performed using the formalism discussed in the present article and in Ref. [17]. The first 100 states of the intermediate nucleus (^{46}Ca) for each allowed spin-parity were considered for TNA calculations.

The variation of the closure and the mixed method NMEs of ^{48}Ca with the closure energy $\langle E\rangle$ for different SRC parametrizations is shown in Fig. 2 and Fig. 3. In these figures, the results are obtained using GXPF1A and GX1R interactions, respectively. It can be discerned from these figures that at optimal $\langle E\rangle$ (where the solid black line crosses dashed red line), the NMEs calculated with mixed method and closure method have the same value. In the case of GXPF1A interaction, the optimal $\langle E\rangle$ are found to be 0.143 MeV for FNS + HOC, 0.356 MeV for CD-Bonn, and 0.209 MeV for AV18 type SRC parametrization. For GX1R interaction, these values are found to be 0.171, 0.399, and 0.252 MeV, respectively. The NMEs obtained at these optimal $\langle E\rangle$ are given in Table II for both the interactions.

Figure 4 shows the dependency of closure NMEs on $\langle E\rangle$. The NMEs are calculated for AV18-type SRC parametrization. It is found that NMEs decrease by about 10% for $\langle E\rangle = 0$ to 10 MeV for both GXPF1A and GX1R interactions. A

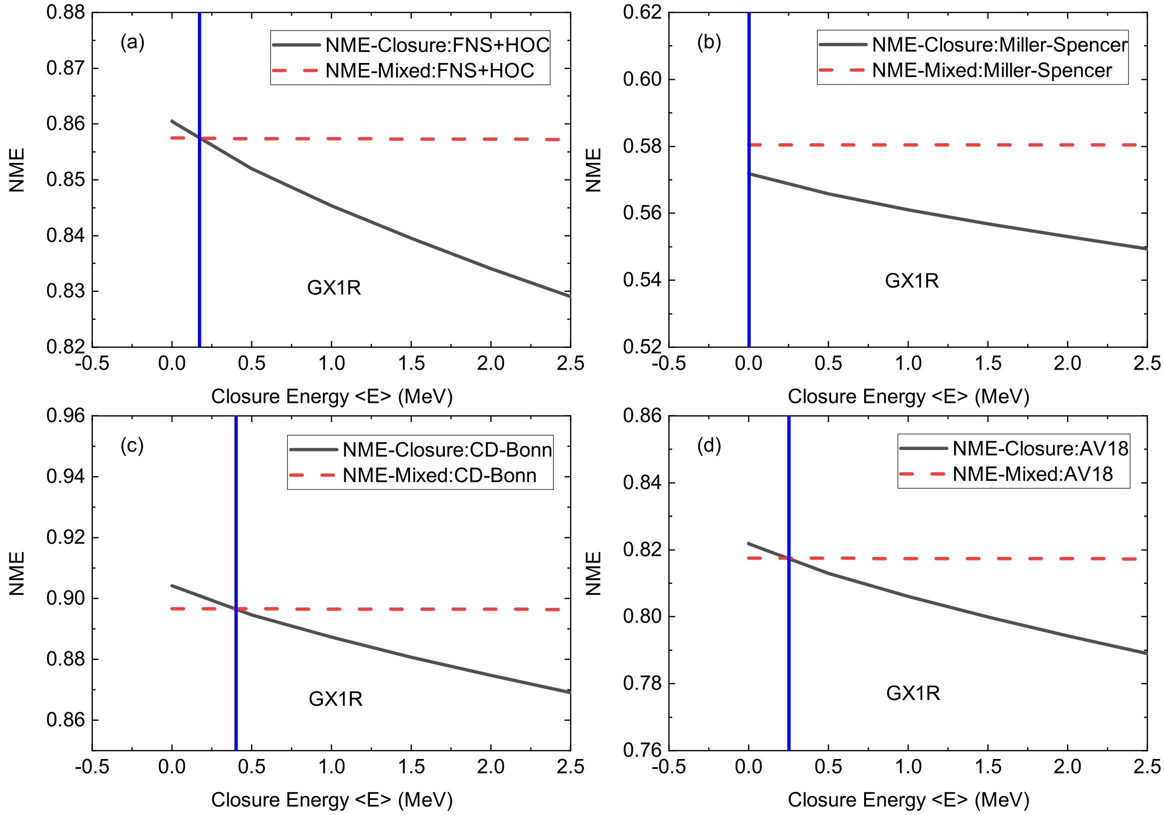

FIG. 3. Dependence of total closure and mixed NME for $0\nu\beta\beta$ (light neutrino-exchange mechanism) of ^{48}Ca on average closure energy $\langle E\rangle$, calculated with GX1R interaction for different SRC parametrization.

similar dependency is also found in our calculations for other SRC parametrizations.

It can also be noted from Fig. 2–4 that the NMEs decreases by less than 1% when $\langle E\rangle = 0.5$ MeV is used at the place of optimal $\langle E\rangle$. Hence, for simplicity, in the rest of our calculations, we have used $\langle E\rangle = 0.5$ MeV. This value of $\langle E\rangle$ was also used in earlier calculations of ^{48}Ca [16–18]. In the present work, with this value of $\langle E\rangle$, we can coherently compare the results for the different components of the GXPF1A and GX1R interactions.

TABLE II. NMEs for $0\nu\beta\beta$ (light neutrino-exchange mechanism) of ^{48}Ca, calculated in closure approximation using optimal values of closure energy $\langle E\rangle$ with GXPF1A and GX1R interaction for different SRC parametrization. Values of $\langle E\rangle$ are in MeV unit.

NME	SRC	$\langle E\rangle$	GXPF1A	$\langle E\rangle$	GX1R
$M_F^{0\nu}$	None	0.143	−0.216	0.171	−0.224
$M_F^{0\nu}$	CD-Bonn	0.356	−0.233	0.399	−0.242
$M_F^{0\nu}$	AV18	0.209	−0.213	0.252	−0.222
$M_{GT}^{0\nu}$	None	0.143	0.778	0.171	0.792
$M_{GT}^{0\nu}$	CD-Bonn	0.356	0.807	0.399	0.823
$M_{GT}^{0\nu}$	AV18	0.209	0.743	0.252	0.756
$M_T^{0\nu}$	None	0.143	−0.077	0.171	−0.074
$M_T^{0\nu}$	CD-Bonn	0.356	−0.079	0.399	−0.076
$M_T^{0\nu}$	AV18	0.209	−0.080	0.252	−0.077
$M^{0\nu}$	None	0.143	0.834	0.171	0.857
$M^{0\nu}$	CD-Bonn	0.356	0.872	0.399	0.896
$M^{0\nu}$	AV18	0.209	0.795	0.252	0.817

The quenching of axial-vector constant g_A in $0\nu\beta\beta$ is an important issue. By using a quenched value of $g_A = 1$ or even much less will have a great effect on NMEs and even greater effects in predicted half-lives of $0\nu\beta\beta$. But, at present, the quenching of axial vector constant g_A in $0\nu\beta\beta$ is still an

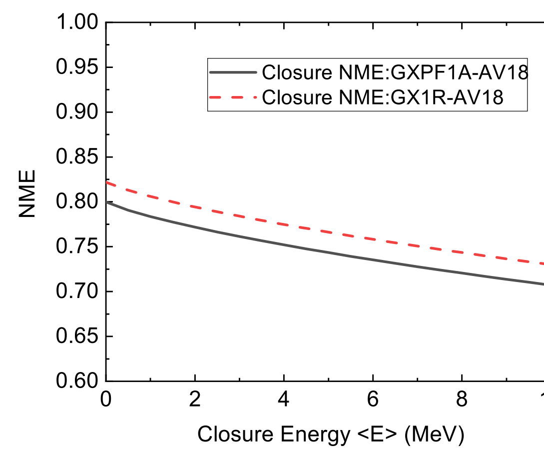

FIG. 4. Variation of NME for $0\nu\beta\beta$ (light neutrino-exchange mechanism) of ^{48}Ca with closure energy $\langle E\rangle$, calculated in closure approximation with total GXPF1A and GX1R interaction for AV18 SRC parametrization.

TABLE III. NMEs calculated with different parts (C, C+SO, and C+SO+T) of GXPF1A and GX1R interaction for $0\nu\beta\beta$ (light neutrino-exchange mechanism) of ^{48}Ca with different SRC parametrization. NMEs are calculated in closure approximation with closure energy $\langle E\rangle =$ 0.5 MeV.

		GXPF1A			GX1R		
NME	SRC	C	C+SO	C+SO+T	C	C+SO	C+SO+T
$M_F^{0\nu}$	None	−0.272	0.232	−0.215	−0.283	0.222	−0.224
$M_F^{0\nu}$	Miller-Spencer	−0.190	0.156	−0.144	−0.198	0.149	−0.150
$M_F^{0\nu}$	CD-Bonn	−0.293	0.250	−0.232	−0.304	0.240	−0.242
$M_F^{0\nu}$	AV18	−0.270	0.229	−0.213	−0.281	0.220	−0.221
$M_{GT}^{0\nu}$	None	0.915	−0.799	0.772	0.981	−0.775	0.787
$M_{GT}^{0\nu}$	Miller-Spencer	0.647	−0.551	0.539	0.703	−0.538	0.546
$M_{GT}^{0\nu}$	CD-Bonn	0.953	−0.834	0.805	1.021	−0.809	0.821
$M_{GT}^{0\nu}$	AV18	0.877	−0.763	0.738	0.941	−0.741	0.752
$M_T^{0\nu}$	None	−0.082	0.071	−0.077	−0.080	0.079	−0.074
$M_T^{0\nu}$	Miller-Spencer	−0.083	0.072	−0.078	−0.082	0.081	−0.075
$M_T^{0\nu}$	CD-Bonn	−0.084	0.073	−0.079	−0.083	0.082	−0.076
$M_T^{0\nu}$	AV18	−0.084	0.073	−0.079	−0.083	0.082	−0.077
$M^{0\nu}$	None	1.002	−0.872	0.828	1.076	−0.834	0.852
$M^{0\nu}$	Miller-Spencer	0.682	−0.575	0.550	0.744	−0.550	0.564
$M^{0\nu}$	CD-Bonn	1.051	−0.916	0.869	1.126	−0.876	0.895
$M^{0\nu}$	AV18	0.960	−0.832	0.791	1.032	−0.796	0.813

open research problem and there is no definitive quenched value of g_A. Hence, in the present calculations, we have used bare value of g_A. In literature different bare value of g_A has been used such as $g_A = 1.25$ [6,15,52], 1.254 [8,16,17], 1.269 [50], and $g_A = 1.27$ [18,53,54]. We have used bare $g_A = 1.27$. With modern bare $g_A = 1.27$, NMEs decreased by less than 1% as compared to NMEs calculated with bare $g_A = 1.25$. Details of the critical issue of quenching of g_A, its value, and its implications in β, $\beta\beta$, and $0\nu\beta\beta$ decays are given in Refs. [13,54–56].

Now we examine the sensitivity of NMEs to the various components (C, SO, and T) of two-nucleon interaction. We have first calculated the NMEs with the C component of both the effective interactions. Then we have calculated them after adding the SO component to the C component. To evaluate the effect of tensor force on NMEs, we have considered the results of the total GXPF1A and GX1R interactions, since $\mathrm{C+SO+T}$ is equal to the total two-nucleon interaction. The NMEs have been calculated by incorporating the effects of FNS, HOC, and SRC. Results for NMEs are summarized in Table III.

For both GXPF1A and GX1R interactions, it is found that the total NMEs calculated with the C part has a positive value. The phase of these NMEs gets changed when they are calculated with the $\mathrm{C+SO}$ part. About 15-18% decrement in the absolute value of the NMEs is also found. This phase shift is once again seen in NMEs when they are calculated with the $\mathrm{C+SO+T}$ (total) part, although in magnitude, NMEs changed by a very small amount. A similar trends of phase shift of NMEs are also observed for Fermi, Gamow-Teller, and tensor type NMEs. Therefore, it can be inferred that the SO and T parts of the two-nucleon interactions negate the effects of each other in NME calculations. For both the interactions, the total NMEs calculated with the C part is found to be 20% enhanced as compared to the NMEs calculated with the total interactions. Further, in GXPF1A and GX1R interaction, there is a little positive push (about 1-3%) in total NMEs for all interaction parts of GX1R interaction. These small changes are due to the different $T = 1$ two-nucleon matrix elements of GX1R interaction.

We further decompose NMEs in terms of partial nuclear matrix elements as a function of coupled spin-parity (J^π) of two decaying neutrons or two created protons:

$$M_\alpha^{0\nu} = \sum_J M_\alpha^{0\nu}(J^\pi), \tag{19}$$

where one can define $M_\alpha^{0\nu}(J^\pi)$ using Eq. (5) as

$$M_\alpha^{0\nu}(J^\pi) = \sum_{k_1'\leqslant k_2', k_1\leqslant k_2} \mathrm{TBTD}(f,i,J^\pi) \times \langle k_1', k_2', J^\pi T|\tau_{-1}\tau_{-2}O_{12}^\alpha|k_1,k_2,J^\pi T\rangle_A. \tag{20}$$

It should be noted that j^π in the above equation also represents the spin-parity of the states of intermediate nucleus ^{46}Ca. The partial NMEs $[M_\alpha^{0\nu}(J^\pi)]$ for each J^π calculated for AV18 SRC parametrization using C, $\mathrm{C+SO}$, and the total two-nucleon interaction are shown in Figs. 5–7, respectively. These figures contain results of both the effective interactions. The dominant contributions in NMEs mostly come from $J^\pi = 0^+$ and 2^+ states. However, it comes with the opposite sign resulting in reduction of total NMEs. It is important to mention that in the dominant contribution of 0^+ and 2^+ states, the bulk part comes from the first 0^+ (ground state) and 2^+ state of ^{46}Ca. A small contribution in NMEs comes from $J^\pi = 4^+$ and

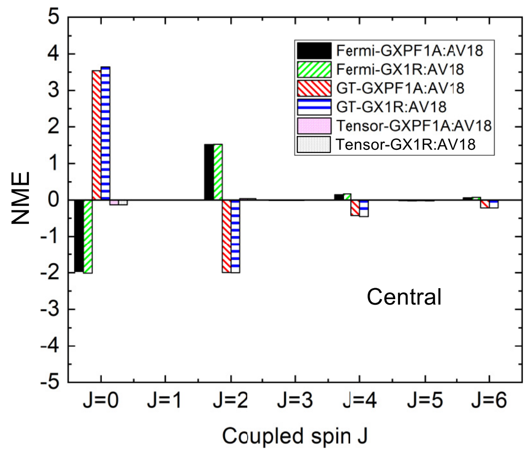

FIG. 5. NMEs for different coupled J^{π} of two initial neutrons or two final protons, calculated with C part of GXPF1A and GX1R interaction for AV18 SRC parametrization with closure energy $\langle E \rangle = 0.5$ MeV.

6^{+} states. There is mostly negligible contributions of odd-J^{+} states to NMEs in comparison to even-J^{+} state. The pairing effect is responsible for such a notable contribution of even-J^{+} states [17]. Similar patterns of dependency of NMEs with J^{π} are also found for other types of SRC parametrizations.

The variation of NMEs with the number of states of the intermediate nucleus can be studied by defining the NMEs as:

$$M_{\alpha}^{0\nu}(N_C) = \sum_{N_m \leqslant N_C} M_{\alpha}^{0\nu}(m), \tag{21}$$

where N_C is the cutoff number of state of intermediate nucleus ^{46}Ca ($|m\rangle$). One can define matrix element $M_{\alpha}^{0\nu}(m)$ using Eq. (5) and Eq. (9) as

$$M_{\alpha}^{0\nu}(m) = \sum_{J,k_1' \leqslant k_2', k_1 \leqslant k_2} \mathrm{TNA}(f, m, k_1', k_2', J)\mathrm{TNA}(i, m, k_1, k_2, J) \times \langle k_1', k_2', JT|\tau_{-1}\tau_{-2}O_{12}^{\alpha}|k_1, k_2, JT\rangle_A. \tag{22}$$

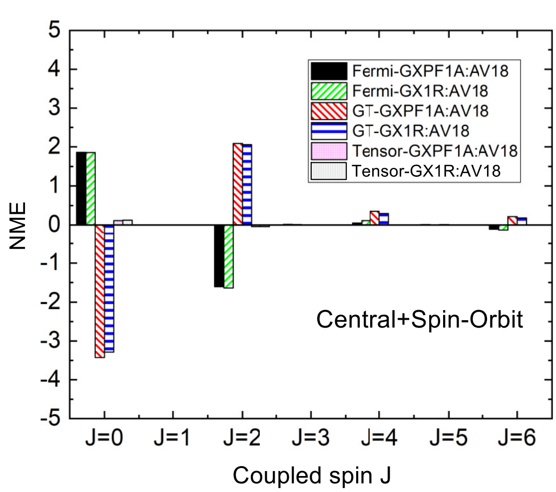

FIG. 6. NMEs for different coupled J^{π} of two initial neutrons or two final protons, calculated with C + SO part of the GXPF1A and GX1R interaction for AV18 SRC parametrization with closure energy $\langle E \rangle = 0.5$ MeV.

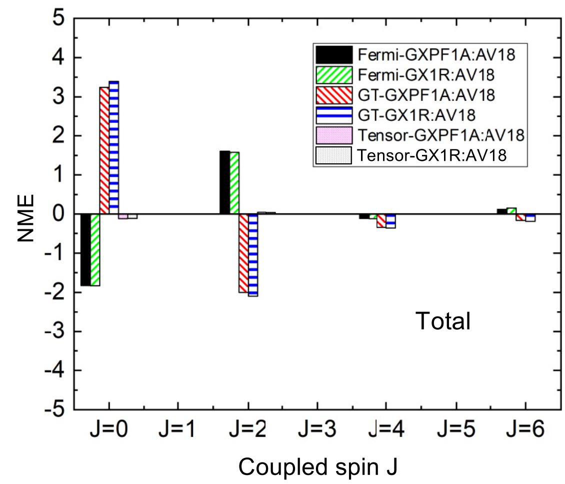

FIG. 7. NMEs for different coupled J^{π} of two initial neutrons or two final protons, calculated with total (C + SO + T) GXPF1A and GX1R interaction for AV18 SRC parametrization with closure energy $\langle E \rangle = 0.5$ MeV.

Figure 8 shows the variation of NMEs with the cutoff number N_C of the states of ^{46}Ca. As an example, we have here presented the results for NMEs with AV18 SRC parametrization. The results are obtained using GXPF1A and GX1R interactions. It is found that the contribution in NMEs mainly comes from the few initial low-lying states. To $N_c = 10$, NMEs keep changing depending on the contribution of each J^{π}. However, NMEs become almost constant at sufficiently large number of states. Thus, it connotes that $N_C = 50$ could be an optimum number to obtain a good TBTD and a constant NME. A similar patterns of variation were also observed in our calculations with C, C + SO, parts of GXPF1A and GX1R interactions, and for other SRC parametarizations.

We have also presented the variations of NMEs with excitation energy of the states of ^{46}Ca. Now the NMEs can be written as a function of cutoff excitation energy of ^{46}Ca states:

$$M_{\alpha}^{0\nu}(E_C) = \sum_{E_m \leqslant E_C} M_{\alpha}^{0\nu}(m), \tag{23}$$

where E_C is the cutoff excitation energy of ^{46}Ca states. The $M_{\alpha}^{0\nu}(m)$ is defined in Eq. (22).

Figure 9 shows the variation of NMEs with the cutoff excitation energy (E_C) of the states of ^{46}Ca. Here we have presented the results for the AV18 type SRC parametrization case, obtained using both the effective interactions. It is found from Fig. 9 that NMEs vary largely up to 10 MeV of exciation energy of ^{46}Ca, and after that, it starts attaining a constant value. Thus, considering states of ^{46}Ca up to $E_C = 15$ MeV is reasonable to obtain a good TBTD and a constant NMEs. The NMEs are less sensitive to high excitation energy states because of the large momentum of the Majorana neutrino (∼100-200 MeV), which is sitting in the denominator of the neutrino potential in Eq. (12).

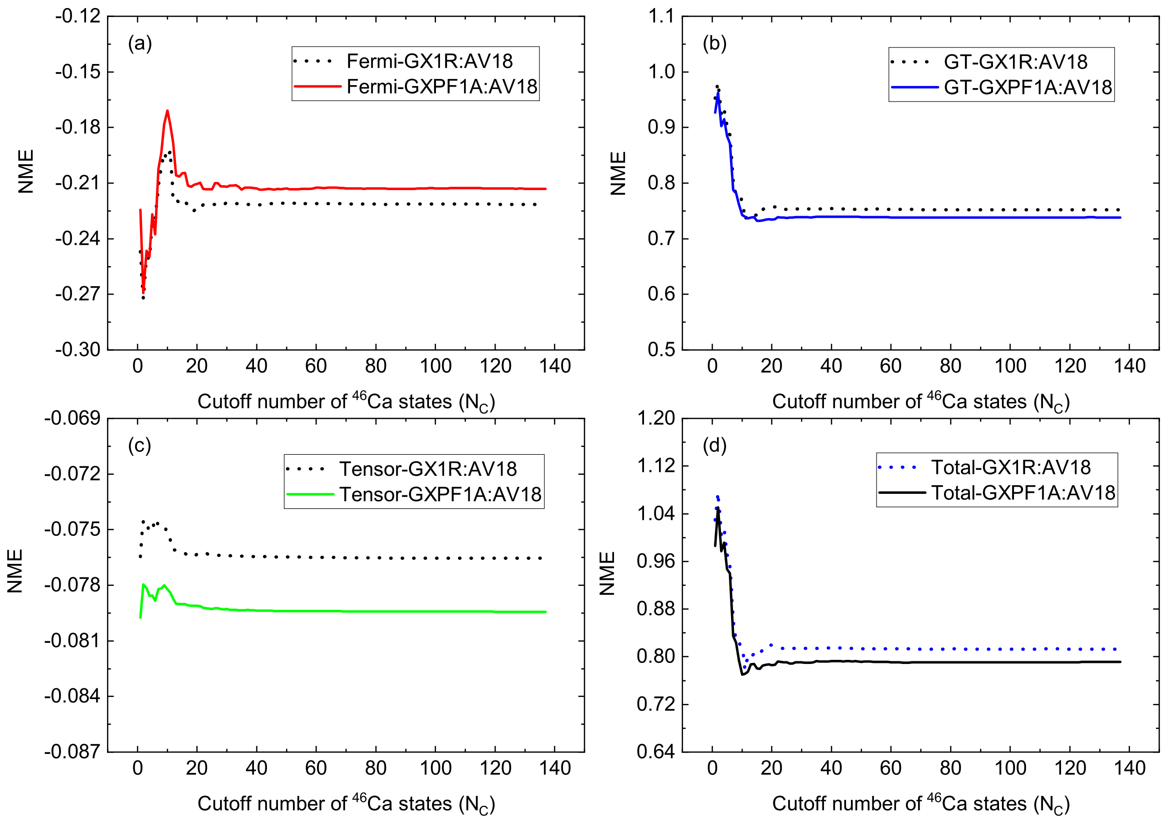

FIG. 8. Variation of NMEs for $0\nu\beta\beta$ of ^{48}Ca with cutoff number of states (N_C) of ^{46}Ca. NMEs are calculated with total GX1R and GXPF1A interaction for AV18 SRC parametrization with closure energy $\langle E\rangle = 0.5$ MeV.

V. SUMMARY AND CONCLUSIONS

We have examined the sensitivity of NMEs for light neutrino-exchange mechanism of $0\nu\beta\beta$ of ^{48}Ca with C, SO, and T components of the GXPF1A interaction and the GX1R, a modified fp model-space interaction. All isospin $T = 1$ tensor force two-nucleon matrix elements and the single-particle energy of $p_{3/2}$ orbital were modified to bring the characteristic properties of tensor force component into new GX1R interaction.

The NMEs were calculated in closure approximation by using the optimal value of closure energy ($\langle E\rangle$). Optimal value of $\langle E\rangle$ was extracted by examining the dependence of closure and mixed NMEs with $\langle E\rangle$ for both the interactions with different SRC parametrizations.

It was found that the total NMEs calculated with the C part of both the interactions is of positive sign. On the addition of SO part to C part, the sign of the total NMEs got changed, and in absolute value NMEs reduced by about 15-18%. The phase shift was also seen in NMEs, calculated by adding the T part to the C + SO part of the interactions. Similar trends of phase shift were observed for Fermi, Gamow-Teller, and tensor matrix elements. Thus, we infer that SO and T parts of the two-nucleon interaction mostly negate the effects of each other in NMEs calculation. The total NMEs, calculated with C part of the interactions were enhanced by about 20% as compared to the NMEs with the total interactions. With new GX1R interaction, about 1-3% increments in the total NMEs were seen as compared to NMEs with GXPF1A interaction for different SRC parametrization. These increments came from the modifications of the isospin $T = 1$ tensor force two-nucleon matrix elements of GX1R interaction to bring the characteristic properties of tensor force into it.

NME for $J^\pi = 0^+$ and 2^+ of two initial neutrons or two final protons dominate the contributions to the total NME, and they come with opposite sign reducing the total NMEs.

We have also presented the variation of NMEs with the number of states and excitation energy of ^{46}Ca, which is used as an intermediate nucleus for calculating TBTD in terms of TNA. It was found that taking first 50 states of ^{46}Ca or states whose excitation energy goes up to 15 MeV is enough to get the accurate value of TBTD, thus a constant NMEs.

ACKNOWLEDGMENTS

S.S. thanks MHRD, Government of India, for the financial support. He is also grateful to Dr. Y. Iwata for the fruitful discussion in calculating two-body matrix elements of the calculations.

APPENDIX A: TWO-BODY MATRIX ELEMENTS OF LIGHT NEUTRINO-EXCHANGE $0\nu\beta\beta$

One can write antisymmetric two-body matrix elements for transition operator O^{α}_{12} of $0\nu\beta\beta$ in nuclear shell

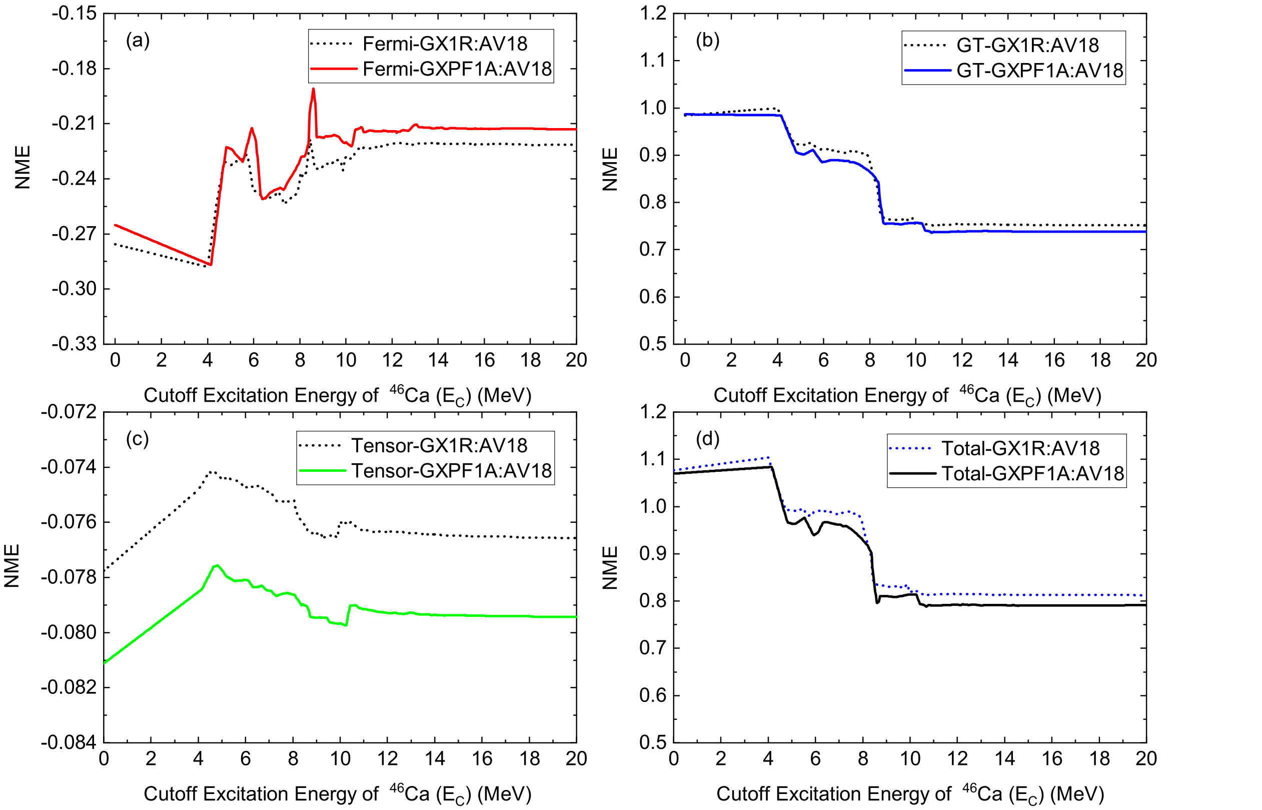

FIG. 9. Variation of NMEs for $0\nu\beta\beta$ of ^{48}Ca with cutoff excitation energy (E_C) of states of ^{46}Ca. NMEs are calculated with total GX1R and GXPF1A interaction for AV18 SRC parametrization with closure energy $\langle E\rangle = 0.5$ MeV.

model as

$$\begin{aligned}
&\langle n_1'l_1'j_1', n_2'l_2'j_2' : JT|\tau_{-1}\tau_{-2}O_{12}^{\alpha}|n_1l_1j_1, n_2l_2j_2 : JT\rangle_A \\
&= \frac{1}{\sqrt{(1+\delta_{j_1'j_2'})[(1+\delta_{j_1j_2})}}(\langle n_1'l_1'j_1', n_2'l_2'j_2' : JT|\tau_{-1}\tau_{-2}O_{12}^{\alpha}|n_1l_1j_1, n_2l_2j_2 : JT\rangle - (-1)^{j_1+j_2+J}\langle n_1'l_1'j_1', n_2'l_2'j_2' : JT| \\
&\quad\times \tau_{-1}\tau_{-2}O_{12}^{\alpha}|n_2l_2j_2, n_1l_1j_1 : JT\rangle], \qquad \text{(A1)}
\end{aligned}$$

where

$$\begin{aligned}
&\langle n_1'l_1'j_1', n_2'l_2'j_2' : J|O_{12}^{\alpha}|n_1l_1j_1, n_2l_2j_2 : J\rangle \\
&= \sum_{S',S}\sum_{\lambda',\lambda}\begin{bmatrix} l_1' & \frac{1}{2} & j_1' \\ l_2' & \frac{1}{2} & j_2' \\ \lambda' & S' & J\end{bmatrix}\begin{bmatrix} l_1 & \frac{1}{2} & j_1 \\ l_2 & \frac{1}{2} & j_2 \\ \lambda & S & J\end{bmatrix}\sum_{n',l',N',L'}\sum_{n,l,N,L}\sum_{\mathcal{J}}\frac{1}{\sqrt{2S+1}}\frac{1}{\sqrt{2\mathcal{J}+1}}U(L',l',J,S':\lambda'\mathcal{J}) \\
&\quad\times U(L,l,J,S:\lambda\mathcal{J})\langle n',l',N',L'|n_1',l_1',n_2',l_2'\rangle_{\lambda'} \\
&\quad\times\langle n,l,N,L|n_1,l_1,n_2,l_2\rangle_{\lambda}\langle l',S':\mathcal{J}||S_{12}^{\alpha}||l,S:\mathcal{J}\rangle\langle n',l'|H_{\alpha}(r)|n,l\rangle. \qquad \text{(A2)}
\end{aligned}$$

One can write in terms of $9j$ symbol

$$\begin{bmatrix} l_1' & \frac{1}{2} & j_1' \\ l_2' & \frac{1}{2} & j_2' \\ \lambda' & S' & J\end{bmatrix} = \sqrt{(2j_1'+1)(2j_2'+1)(2\lambda'+1)(2S'+1)}\times\begin{Bmatrix} l_1' & \frac{1}{2} & j_1' \\ l_2' & \frac{1}{2} & j_2' \\ \lambda' & S' & J\end{Bmatrix}. \qquad \text{(A3)}$$

In terms of the $6j$ symbol one can write

$$U(L',l',J,S':\lambda'\mathcal{J}) = (-1)^{L'+l'+S'+J}\sqrt{2\lambda'+1}\sqrt{2\mathcal{J}+1}\begin{Bmatrix} L' & l' & \lambda' \\ S' & J & \mathcal{J}\end{Bmatrix}. \qquad \text{(A4)}$$

$\langle n',l',N',L'|n_1',l_1',n_2',l_2'\rangle_{\lambda'}$ is the harmonic oscillator bracket used to convert the radial integral of neutrino potential from individual coordinate system of nucleons to relative and center of mass coordinate system of the nucleons.

APPENDIX B: FORM FACTORS

Form factors that include the higher-order terms in the nucleon currents are given by [7,42]

$$h_F(q^2) = g_V^2(q^2), \tag{B1}$$

$$h_{\mathrm{GT}}(q^2) = \frac{g_A^2(q^2)}{g_A^2}\left[1 - \frac{2}{3}\frac{q^2}{q^2+m_\pi^2} + \frac{1}{3}\left(\frac{q^2}{q^2+\pi^2}\right)^2\right] + \frac{2}{3}\frac{g_M^2(q^2)}{g_A^2}\frac{q^2}{4m_p^2}, \tag{B2}$$

$$h_T(q^2) = \frac{g_A(q^2)}{g_A^2}\left[\frac{2}{3}\frac{q^2}{q^2+m_\pi^2} - \frac{1}{3}\left(\frac{q^2}{q^2+m_\pi^2}\right)^2\right] + \frac{1}{3}\frac{g_M^2(q^2)}{g_A^2}\frac{q^2}{4m_p^2}. \tag{B3}$$

The effects of FNS are included with $g_V(q)^2$, $g_A(q^2)$, and $g_M(q^2)$ form factors, which, in the dipole approximation, are given by [15]

$$g_V(q^2) = \frac{g_V}{\left(1+\frac{q^2}{M_V^2}\right)^2}, \tag{B4}$$

$$g_A(q^2) = \frac{g_A}{\left(1+\frac{q^2}{M_A^2}\right)^2}, \tag{B5}$$

$$g_M(q^2) = (\mu_p - \mu_n)g_V(q^2). \tag{B6}$$

$\mu_p - \mu_n = 4.7$, $M_V = 850$ MeV, $M_A = 1086$ MeV; m_p and m_π are the mass of protons and pions.

[1] J. Schechter and J. W. F. Valle, Neutrinoless double-β decay in su(2) $\times$ u(1) theories, Phys. Rev. D **25**, 2951 (1982).

[2] T. Tomoda, Double beta decay, Rep. Prog. Phys. **54**, 53 (1991).

[3] F. T. Avignone, S. R. Elliott, and J. Engel, Double beta decay, majorana neutrinos, and neutrino mass, Rev. Mod. Phys. **80**, 481 (2008).

[4] F. F. Deppisch, M. Hirsch, and H. Päs, Neutrinoless double-beta decay and physics beyond the standard model, J. Phys. G: Nucl. Part. Phys. **39**, 124007 (2012).

[5] W. Rodejohann, Neutrino-less double beta decay and particle physics, Int. J. Mod. Phys. E **20**, 1833 (2011).

[6] V. Rodin, A. Faessler, F. Šimkovic, and P. Vogel, Assessment of uncertainties in qrpa $0\nu\beta\beta$-decay nuclear matrix elements, Nucl. Phys. A **766**, 107 (2006).

[7] F. Šimkovic, G. Pantis, J. D. Vergados, and A. Faessler, Additional nucleon current contributions to neutrinoless double β decay, Phys. Rev. C **60**, 055502 (1999).

[8] J. D. Vergados, H. Ejiri, and F. Šimkovic, Theory of neutrinoless double-beta decay, Rep. Prog. Phys. **75**, 106301 (2012).

[9] R. N. Mohapatra and G. Senjanović, Neutrino Mass and Spontaneous Parity Nonconservation, Phys. Rev. Lett. **44**, 912 (1980).

[10] R. N. Mohapatra and J. D. Vergados, New Contribution to Neutrinoless Double Beta Decay in Gauge Models, Phys. Rev. Lett. **47**, 1713 (1981).

[11] R. N. Mohapatra, New contributions to neutrinoless double-beta decay in supersymmetric theories, Phys. Rev. D **34**, 3457 (1986).

[12] J. Vergados, Neutrinoless double β-decay without majorana neutrinos in supersymmetric theories, Phys. Lett. B **184**, 55 (1987).

[13] J. Engel and J. Menéndez, Status and future of nuclear matrix elements for neutrinoless double-beta decay: A review, Rep. Prog. Phys. **80**, 046301 (2017).

[14] E. Caurier, J. Menéndez, F. Nowacki, and A. Poves, Influence of Pairing on the Nuclear Matrix Elements of the Neutrinoless $\beta\beta$ Decays, Phys. Rev. Lett. **100**, 052503 (2008).

[15] M. Horoi and S. Stoica, Shell model analysis of the neutrinoless double-β decay of ^{48}Ca, Phys. Rev. C **81**, 024321 (2010).

[16] R. A. Sen'kov and M. Horoi, Neutrinoless double-β decay of ^{48}ca in the shell model: Closure versus nonclosure approximation, Phys. Rev. C **88**, 064312 (2013).

[17] B. A. Brown, M. Horoi, and R. A. Sen'kov, Nuclear Structure Aspects of Neutrinoless Double-β Decay, Phys. Rev. Lett. **113**, 262501 (2014).

[18] Y. Iwata, N. Shimizu, T. Otsuka, Y. Utsuno, J. Menéndez, M. Honma, and T. Abe, Large-Scale Shell-Model Analysis of the Neutrinoless $\beta\beta$ Decay of ^{48}Ca, Phys. Rev. Lett. **116**, 112502 (2016).

[19] J. Barea and F. Iachello, Neutrinoless double-β decay in the microscopic interacting boson model, Phys. Rev. C **79**, 044301 (2009).

[20] J. Barea, J. Kotila, and F. Iachello, Limits on Neutrino Masses from Neutrinoless Double-β Decay, Phys. Rev. Lett. **109**, 042501 (2012).

[21] T. R. Rodríguez and G. Martínez-Pinedo, Energy Density Functional Study of Nuclear Matrix Elements for Neutrinoless $\beta\beta$ Decay, Phys. Rev. Lett. **105**, 252503 (2010).

[22] L. S. Song, J. M. Yao, P. Ring, and J. Meng, Relativistic description of nuclear matrix elements in neutrinoless double-β decay, Phys. Rev. C **90**, 054309 (2014).

[23] P. K. Rath, R. Chandra, K. Chaturvedi, P. K. Raina, and J. G. Hirsch, Uncertainties in nuclear transition matrix elements for neutrinoless $\beta\beta$ decay within the projected-Hartree-Fock-Bogoliubov model, Phys. Rev. C **82**, 064310 (2010).

[24] P. Kumar, K. Jha, P. K. Raina, and P. P. Singh, Quasi shell gap at ^{23}F, Nucl. Phys. A **983**, 210 (2019).

[25] P. Kumar, S. Sarkar, P. P. Singh, and P. K. Raina, Proton-neutron force and proton single-particle strength in Sc, F, and Li isotopes, Phys. Rev. C **100**, 024328 (2019).

[26] A. Umeya and K. Muto, Triplet-even channel attraction for shell gaps, Phys. Rev. C **69**, 024306 (2004).

[27] A. Umeya and K. Muto, Single-particle energies in neutron-rich nuclei by shell model sum rule, Phys. Rev. C **74**, 034330 (2006).
[28] N. A. Smirnova, K. Heyde, B. Bally, F. Nowacki, and K. Sieja, Nuclear shell evolution and in-medium *nn* interaction, Phys. Rev. C **86**, 034314 (2012).
[29] J. P. Elliott *et al.*, Matrix elements of the nucleon-nucleon potential for use in nuclear-structure calculations, Nucl. Phys **121**, 241 (1968).
[30] M. W. Kirson, Spin-tensor decomposition of nuclear effective interactions, Phys. Lett. B **47**, 110 (1973).
[31] J. P. Schiffer and W. W. True, The effective interaction between nucleons deduced from nuclear spectra, Rev. Mod. Phys. **48**, 191 (1976).
[32] K. Klingenbeck, W. Knüpfer, M. G. Huber, and P. W. M. Glaudemans, Central and noncentral components of the effective sd-shell interaction, Phys. Rev. C **15**, 1483 (1977).
[33] Y. Kenji, Spin-tensor decomposition of effective interactions for 0p shell nuclei, Nucl. Phys. A **333**, 67 (1980).
[34] N. Smirnova, B. Bally, K. Heyde, F. Nowacki, and K. Sieja, Shell evolution and nuclear forces, Phys. Lett. B **686**, 109 (2010).
[35] B. Brown, W. Richter, and B. Wildenthal, Spin-tensor analysis of a new empirical shell-model interaction for the 1s-0d shell nuclei, J. Phys. G **11**, 1191 (1985).
[36] B. Brown, W. Richter, R. Julies, and B. Wildenthal, Semi-empirical effective interactions for the 1s-od shell, Ann. Phys. **182**, 191 (1988).
[37] E. Osnes and D. Strottman, Spin-tensor analysis of realistic shell model interactions, Phys. Rev. C **45**, 662 (1992).
[38] M. Honma, T. Otsuka, B. A. Brown, and T. Mizusaki, New effective interaction for pf-shell nuclei and its implications for the stability of the $n = z = 28$ closed core, Phys. Rev. C **69**, 034335 (2004).
[39] M. Honma, T. Otsuka, B. Brown, and T. Mizusaki, Shell-model description of neutron-rich pf-shell nuclei with a new effective interaction gxpf1, Eur. Phys. J. A **25**, 499 (2005).
[40] K. Jha, P. Kumar, S. Sarkar, and P. K. Raina, Modification of effective interaction in pf-shell using spin-tensor decomposition, arXiv:1908.07983v2 (2019).
[41] J. Kotila and F. Iachello, Phase-space factors for double-β decay, Phys. Rev. C **85**, 034316 (2012).
[42] F. Šimkovic, A. Faessler, H. Müther, V. Rodin, and M. Stauf, $0\nu\beta\beta$-decay nuclear matrix elements with self-consistent short-range correlations, Phys. Rev. C **79**, 055501 (2009).
[43] https://www.nndc.bnl.gov.
[44] T. Otsuka, T. Suzuki, M. Honma, Y. Utsuno, N. Tsunoda, K. Tsukiyama, and M. Hjorth-Jensen, Novel Features of Nuclear Forces and Shell Evolution in Exotic Nuclei, Phys. Rev. Lett. **104**, 012501 (2010).
[45] N. Tsunoda, T. Otsuka, K. Tsukiyama, and M. Hjorth-Jensen, Renormalization persistency of the tensor force in nuclei, Phys. Rev. C **84**, 044322 (2011).
[46] T. Otsuka, T. Suzuki, R. Fujimoto, H. Grawe, and Y. Akaishi, Evolution of Nuclear Shells due to the Tensor Force, Phys. Rev. Lett. **95**, 232502 (2005).
[47] M. Honma, T. Otsuka, and T. Mizusaki, Shell-model description of neutron-rich ca isotopes, RIKEN Accel. Prog. Rep. **41**, 32 (2008).
[48] B. Brown and W. Rae, The shell-model code nushellx@ msu, Nucl. Data Sheets **120**, 115 (2014).
[49] R. A. Sen'kov and M. Horoi, Accurate shell-model nuclear matrix elements for neutrinoless double-β decay, Phys. Rev. C **90**, 051301(R) (2014).
[50] R. A. Sen'kov and M. Horoi, Shell-model calculation of neutrinoless double-β decay of ^{76}Ge, Phys. Rev. C **93**, 044334 (2016).
[51] R. A. Sen'kov, M. Horoi, and B. A. Brown, Neutrinoless double-β decay of ^{82}Se in the shell model: Beyond the closure approximation, Phys. Rev. C **89**, 054304 (2014).
[52] F. Šimkovic, A. Faessler, V. Rodin, P. Vogel, and J. Engel, Anatomy of the $0\nu\beta\beta$ nuclear matrix elements, Phys. Rev. C **77**, 045503 (2008).
[53] J. Suhonen, Impact of the quenching of g_A on the sensitivity of $0\nu\beta\beta$ experiments, Phys. Rev. C **96**, 055501 (2017).
[54] J. T. Suhonen, Value of the axial-vector coupling strength in β and $\beta\beta$ decays: A review, Front. Phys. **5**, 55 (2017).
[55] I. S. Towner, Quenching of spin matrix elements in nuclei, Phys. Rep. **155**, 263 (1987).
[56] T.-S. Park, H. Jung, and D.-P. Min, In-medium effective axial-vector coupling constant, Phys. Lett. B **409**, 26 (1997).